Journal of Sound and Vibration (1999) **225**(1), 95–109
Article No. jsvi.1999.2231, available online at http://www.idealibrary.com on IDEAL®

DYNAMIC STUDY OF A SIMPLIFIED MECHANICAL SYSTEM WITH PRESENCE OF DRY FRICTION

A. TOUFINE

ENSAE, 10 *Avenue Edouard Belin*, 31055 *Toulouse*, *France*

J. J. BARRAU

LGMT/UPS, 118 *Route de Narbonne*, 31400 *Toulouse*, *France*

AND

M. BERTHILLIER

SNECMA Villaroche, 77550 *Moissy Cramayel*, *France*

(*Received* 20 *July* 1998, *and in final form* 15 *February* 1999)

In aero engines, amplitudes of blade vibrations are frequently reduced by centrifugal flyweights, called friction peak limiters, which exert a dry friction force under the blade platforms. To understand the physical phenomena which cause reduction of vibration amplitudes, a system comprising two degrees of freedom, but generally representative of a real system, is studied. It is shown that system response can be found by analyzing the sliding and the stuck state. It appears therefore that the most important phenomenon controlling movement is the change of boundary conditions. In addition, the effect of other parameters is analyzed. The effect of a large difference between the fundamental frequencies is demonstrated as well as the influence of the dynamic friction coefficient for lengthening the plateau of the efficiency curve. All these results can be used to improve numerical methods of resolution.

1. INTRODUCTION

In aero engines, aeroelastic coupling effects can cause large displacements and severe stresses in the structure. Fluctuating stresses, even of moderate intensity, may thus cause material failure through fatigue. The engineer must therefore find suitable devices to control vibration in the system. One such device currently used in aero engines to limit these vibrations consists of a centrifugal flyweight that creates a dry friction contact under two adjacent blade platforms (Figure 1). This system will be called "dry friction peak limiter" in this paper.

Friction damping has received considerable attention from a number of researchers. Hartog [1] and Hundal [2] determined the response of a single-degree-of-freedom system with a rigid friction damper subjected to harmonic excitation. However, in the case of a multiple degree of freedom, the

0022-460X/99/310095 + 15 $30.00/0

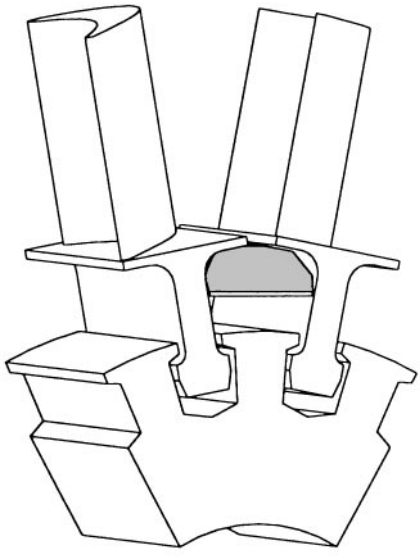

Figure 1. Blade with dry friction system.

number of simultaneous equations to be solved becomes prohibitively large and the method is inefficient. Time integration can be applied but, for very low damping levels, these methods can be computationally expensive. Griffin [3], Ostachowicz [4], Dowell and Schartz [5, 6] used the harmonic balance method. Although this method is efficient, its results are accurate only for continuous slip motion since the response is limited to a single harmonic approximation. Ferri [7] and Ferri and Dowell [8] applied the technique of the multi-harmonic frequency domain solution to analyze the steady state response of a system with dry friction. This method, compared with time integration, produces very good results, showing that the effect of higher harmonics is significant when stick-slip motion occurs. Cameron and Griffin [9] Cardonna *et al.* [10] have improved the numerical efficiency of this method by the introduction of the FFT algorithm.

Most analyses consider the friction interface to be constrained to one-dimensional motion. For contact at a point, a macro-slip model is sufficient [11] but when the friction contact is large, a micro-slip model [12], in which only a part of the interface may be slipping while the other part remains stuck, is necessary. This micro-slip model is also necessary in applications where the assumption of one-dimensional motion is not valid. This is the case for turbine blades where there is often coupling between motion of the structure such as bending and torsion. Toufine *et al.* [13] analyze this problem by considering that the direction of the sliding motion is known. Menq *et al.* [14] and Sanliturk and Ewins [15] analyze the general case of elliptical motion across a friction interface with constant normal force.

To apply these methods to industrial cases with many degrees of freedom, it is necessary to reduce the size of the system. Dowell [5] proposed a component mode analysis with the mode of the structure without dampers. Kormarz *et al.* [11] used

the modal effective parameters, as defined by Girard and Roy [16], which allow a comprehensive description of the eigenmodes and the control of the truncation effects. Berthillier *et al.* and Touffine *et al.* [17,18] preferred the Craig–Bampton component mode synthesis where the retained degree of freedom included those where frictional force is applied. This technique is particularly interesting because the mass and stiffness matricés can easily be obtained from a finite-element code.

The conclusions of all these studies are generally similar: the friction peak limiter efficiency is limited to a range of excitation forces corresponding to stick and slip in the friction zone.

Although studies generally correlate well with experimental results, they do not answer the following important questions:

— what is the physical origin of the limitation of the displacement response of a dry friction system?
— is energy dissipation by the dry friction system the principal parameter governing system response?
— why does discontinuity appear on the response curve at some excitation force amplitudes?
— what is the importance of the different parameters?

The aim of this present study is to answer these questions by analyzing a simplified mechanical system, comprising only two degrees of freedom, but generally representative of a real problem.

To verify our hypothesis and proposed methods, a complete non-linear study has been carried out and used as a reference.

2. STUDY OF THE SIMPLIFIED SYSTEM

2.1. PHYSICAL DESCRIPTION

To determine the dynamic behaviour of a real structure, the finite-element method is generally used and to achieve the numerical resolution of equations of motion in the case of a non-linear system the size of the model must be reduced. For example, Korkmaz *et al.* [11] use the modal effective parameters and divide the structure into two parts:

(1) Between the clamped end and the dry friction contact point, which is modelled by a beam with two degrees of freedom;
(2) From the contact zone up to the free end, which is modelled by the modal effective parameters, also with two degrees of freedom.

By analogy, the mechanical system analyzed in this paper is reduced to two degrees of freedom. While Korkmaz *et al.* [11] has employed a lateral model to analyze the bending mode, in this article we have used an axial model which has the same overall dynamic behaviour. In this model two spring–mass–dampers are connected in series where the rigid masses m_2 and m_1 are both assumed to move along the same horizontal line. The individual masses can be located at any time by the two co-ordinates X_2 and X_1. Thus the system has two degrees of freedom. The massless spring has a linear force deflection relationships denoted by the spring

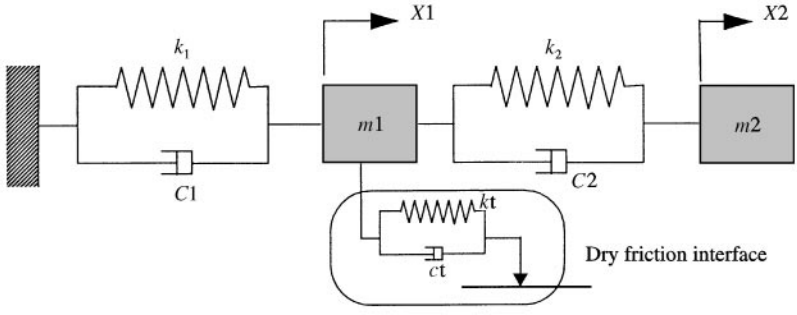

Figure 2. Two degrees of freedom model. $m_1 = 0{\cdot}9$ Kg, $m_2 = 1{\cdot}3$ Kg, $c_1 = c_2 = 2{\cdot}53$ Ns/m, $c_t = 10^{-4}$ Ns/m, $k_1 = 6 \times 10^5$ N/m, $k_2 = 2 \times 10^5$ N/m, $k_t = 7 \times 10^7$ N/m $\mu = 0{\cdot}4$.

constants k_2 and k_1. Similarly, the massless dampers exhibit linear force–velocity relationships denoted by the damping coefficients c_2 and c_1. Mass m_1 is subjected to a dry friction force. The system comprising k_1, m_1 and c_1 represents the blade root. Similarly, the system comprising k_2, m_2, c_2, represents the outer part of the blade. The system is loaded by an excitation force $Pi(t) = P\sin(\omega t)$ acting on mass m_2 where P denotes the amplitude and ω the frequency. The different parameter values are indicated in Figure 2.

2.2. DRY FRICTION MODELLING

Ferrero and Barrau [19] show that, for small displacements at low speeds, a friction link can correctly be represented:

— in the stuck state: by spring of stiffness k_t and a viscous damper c_t which represent the asperity junction. The stiffness value k_t is a function of the normal contact force F_N;
— in the sliding state: by a dry runner characterized by a dynamic friction coefficient μ_d.

The transition from one state to the other is governed by the value of the static coefficient μ_s, which depends on the previous states. After several stuck phases of short duration, Ferrero and Barrau [19] show that the static coefficient value tends towards the dynamic coefficient value denoted by μ_d.

Since in this problem the duration of stuck phases is very short, the dry runner releasing threshold will thus be equal to μ_d. F_N and μ_d will be supposed constant. Moreover, for aero engine blades the normal force F_N is created by the centrifugal force and does not vary, in which case the two parameters k_t and c_t can be considered constant. The dry friction law used is similar to the one used by Korkmaz *et al.*, [11] as described by the following relations:

$$F_T = \mu_d \frac{\dot{X}}{|\dot{X}|} F_N \quad \text{if } F_{int} > \mu_d F_N \text{ during sliding state,} \tag{1}$$

$$F_T = F_{int} = k_t(X - X_{fix}) + c_t\dot{X} \quad \text{if } F_{int} < \mu_d F_N \text{ during stuck state,} \tag{2}$$

where F_T denotes the tangential force and F_{int} is the interface force.

In these relationships, X is the relative speed at the friction contact point and X_{fix} is a parameter ensuring the continuity of the tangential force between the stuck and sliding states. Wang and Shieh [20] and Anderson and Ferri [21] consider the case where the normal force is variable.

3. CONVENTIONAL NON-LINEAR RESOLUTION OF THE SIMPLIFIED SYSTEM

To form a basis for comparison and also to validate our methodological approach, a complete non-linear study has been carried out from methods developed by Korkmaz *et al.* [11] and Toufine *et al.* [13] and verified experimentally by these authors.

3.1. METHODOLOGY

The problem has been resolved by direct integration of the equations of motion using the Newmark method. Initially, it is supposed that the friction interface is in a stuck phase. At each interval of time, the interface force F_{int} is compared to the dry friction effort $\mu_d \cdot F_N$ (equation (1)) to analyze the friction interface state.

The exact instant where the system passes from one phase to another is found accurately by using the Golden Section method [22]. The tangential force continuity is carried out by determining the value X_{fix} (equation (2)).

System response can thus be obtained for a given excitation force.

3.2. BRIEF BEHAVIOUR ANALYSIS OF THE SYSTEM

These calculations must be carried out for various amplitudes of the exciting force and for different frequencies. It is possible then to determine:

— For one amplitude of the excitation force, the relationship between the amplitude of masses m_1 or m_2 and the excitation frequency (see Figure 3).
— The relationship between the displacement maximum of mass m_2 and the amplitude of the exciting force whatever the excitation frequency. Each point of this curve is then associated with a different frequency. This curve will be called "friction peak limiter efficiency curve" and is derived from the maximum points on the preceding curves.

Fortunately, these calculations only need to be made for one normal force F_N since the governing equations can be non-dimensionalized by the variable F_N.

On the "friction peak limiter efficiency" curve, the three behaviour zones, indicated by the different authors, can be clearly observed in Figure 4 :

— the first zone AB, where the displacement–force relationship is linear;
— the second zone BC, which has the appearance of a plateau. This zone corresponds to the optimum efficiency of the friction peak limiter;

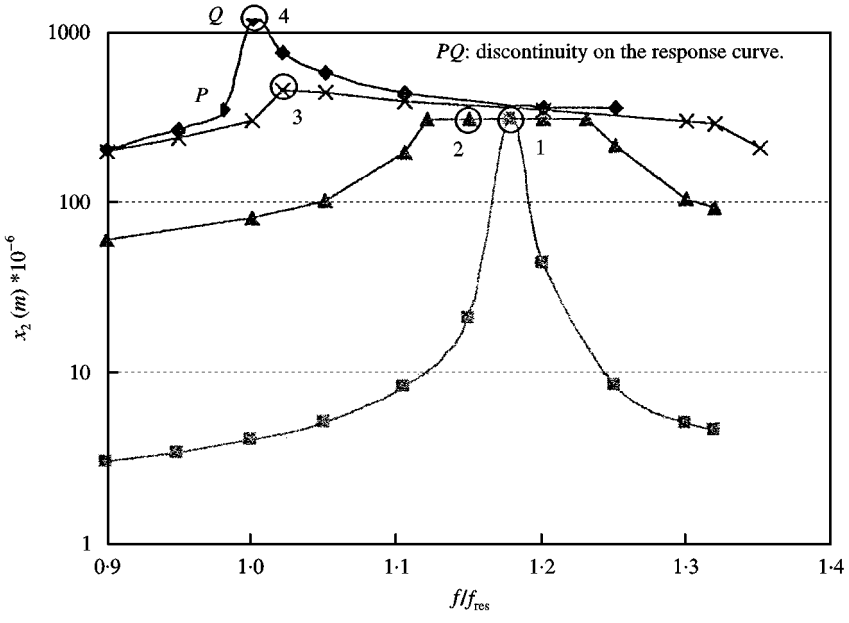

Figure 3. Variation of the amplitude X_2 with frequency ratio and excitation forces: —■— $P = 0{\cdot}22$ N; —▲— $P = 4{\cdot}5$ N; —×— $P = 12$ N; —◆— $P = 13{\cdot}5$ N.

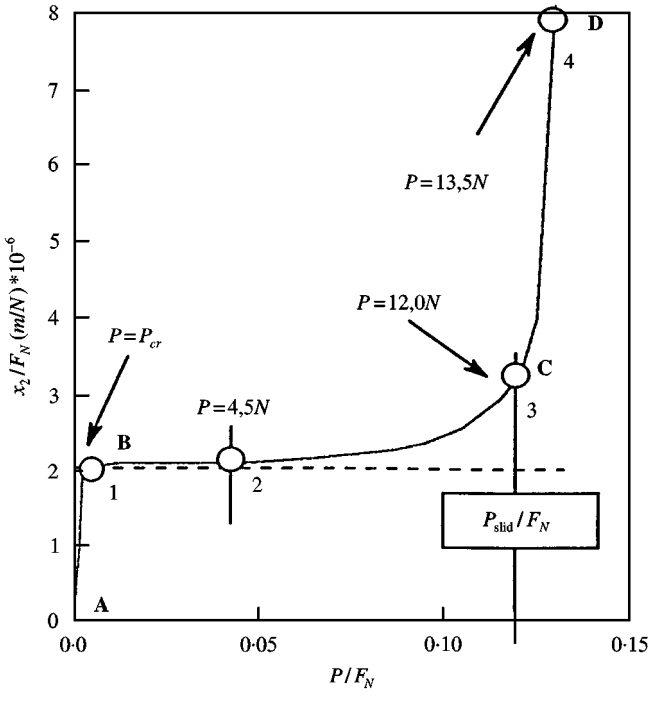

Figure 4. Friction peak limiter efficiency curve. — Variable frequency

— the third and last zone CD, where amplitude of the displacement increases quickly.

Thus this system can be considered representative of a real system.

4. MOVEMENT SYSTEM ANALYSIS BY LIMITED STATES

In the numerical resolution, one system is in fact studied with two different boundary conditions. Thus, complete movement is analyzed solely from the knowledge of the following two limited states:

- permanently stuck friction interface;
- permanently sliding friction interface.

The resolution associated with the stuck state does not present any difficulties, since this problem is linear. The fundamental frequency of the stuck mode will be called f_1 and the curve response C_1.

In the second state, the solution is determined by decomposing the displacements and applied forces in Fourier Series and by keeping only the first harmonic:

$$P(t) = P \cdot \sin(\omega t),$$

$$x(t) = X \cdot \cos(\omega t + \phi) \tag{3}$$

$$\Rightarrow C_{\text{eq}} = \frac{4\mu_{\text{d}} \cdot F_{\text{N}}}{\pi \cdot \omega \cdot X}. \tag{4}$$

Thus, the dry friction force $\mu_{\text{d}} F_{\text{N}} \cdot \dot{X}/(|\dot{X}|)$ is replaced by an equivalent damping coefficient C_{eq} with the value indicated in equation (4). If the response amplitude X is taken at the preceding frequency, the problem becomes linear. The fundamental frequency of the sliding mode will be denoted by f_2 and the curve response by C_2.

Let us analyze the force-displacement responses of these two systems, for a given amplitude of the excitation force, and over a frequency range including the sliding frequency mode and the stuck frequency mode.

At this stage, it is interesting to note, on these response curves shown in Figure 5, two characteristic points I and S that play a very important role in the analysis:

— I is the intersection point between the two curves;
— S is the maximum of curve C_1.

Ordinates of points I and S are respectively denoted by X_{I} and X_{s}.

4.1. FIRST CONFIGURATION OF LOADING

Firstly, let us analyze this system in a stuck state. In this case, the effort exerted on the mass m_1 by the friction peak limiter is proportional to X_1, but also to the excitation force P since the system is linear. The interface force will be maximum for an excitation frequency $f = f_1$. Let us call P_{cr} the external force which, for an

excitation frequency equal to f_1 creates a displacement of the mass m_1, X_{1cr}, such that:

$$X_{1cr} = \mu_s F_N / k_t. \tag{5}$$

For this force P_{cr} and this frequency f_1, the mass m_2 displacement is noted X_{2cr}.

If the force P is less than P_{cr}, whatever the excitation frequency, and since the behaviour is linear, the displacement X_1 will be less than X_{1cr}. The interface force will therefore be less than the limited value $\mu_S \cdot F_N$ and the non-sliding hypothesis is correct.

The P_{cr} force value will be called "critical sliding force". With the chosen parameters, P_{cr} has the value of 0·22 N.

For an excitation force P in the range $[0, P_{cr}]$, the peak limiter efficiency curve must be a straight line and its gradient is given by the viscous damping coefficient (see Figure 8(a)). The non-linear method obviously gives the same result. This portion of curve is valid only if the displacement X_1 is less than $\mu_S \cdot F_N / k_t$ so the end of this phase is directly linked to the value of μ_S.

4.2. SECOND LOADING CONFIGURATION: P SUPERIOR TO P_{CR}

Now consider a loading amplitude, such that points S and I are situated on either side of the critical value X_{2cr}, represented by the straight line L (see Figure 5). B and C are the two points of curve C_1 which has X_{2cr} for ordinate.

Let f_B and f_C be the excitation frequencies associated with B and C. The response of the system, must now be studied as a function of the excitation frequency.
If the excitation frequency is less than f_B or greater than f_C, the displacement of the mass m_2 is less than X_{2cr} and therefore the system remains in a stuck state. The response must be given by parts AB and CD of the curve C_1 as illustrated in Figure 5.

For frequencies lower than f_B, one question remains: can the system jump, after an external perturbation, in the sliding mode? In fact, this is not possible since there will always be an instant t at which the speed of mass m_1 vanishes. At this moment, boundaries conditions are those of the stuck state and the system will remain in this state since the displacement is less than X_{2cr}.

This mechanical system cannot therefore have a bi-stable behaviour at these frequencies. If the excitation frequency lies between f_B and f_C, the displacement X_1 is greater than X_{1cr}. The force exerted by the spring k_t (Figure 2), will then be greater than $\mu_S \cdot F_N$ and the system should slide (point B).

The response would be represented by the curve C_2 in Figure 5, but in this case of force, the mode generates vibration amplitudes lower than the critical value X_{2cr}. Therefore, the system cannot remain in this state. It must pass successively from a stuck to a sliding state, and maximum amplitude will be limited to the value X_{2cr}.

The path taken by the system for a frequency in the interval $[f_B, f_C]$, should be represented by the segment BC in Figure 5.

If these results are compared to those given by the complete non-linear analysis, the response curve is exactly the same (see Figure 5), which validates this limited

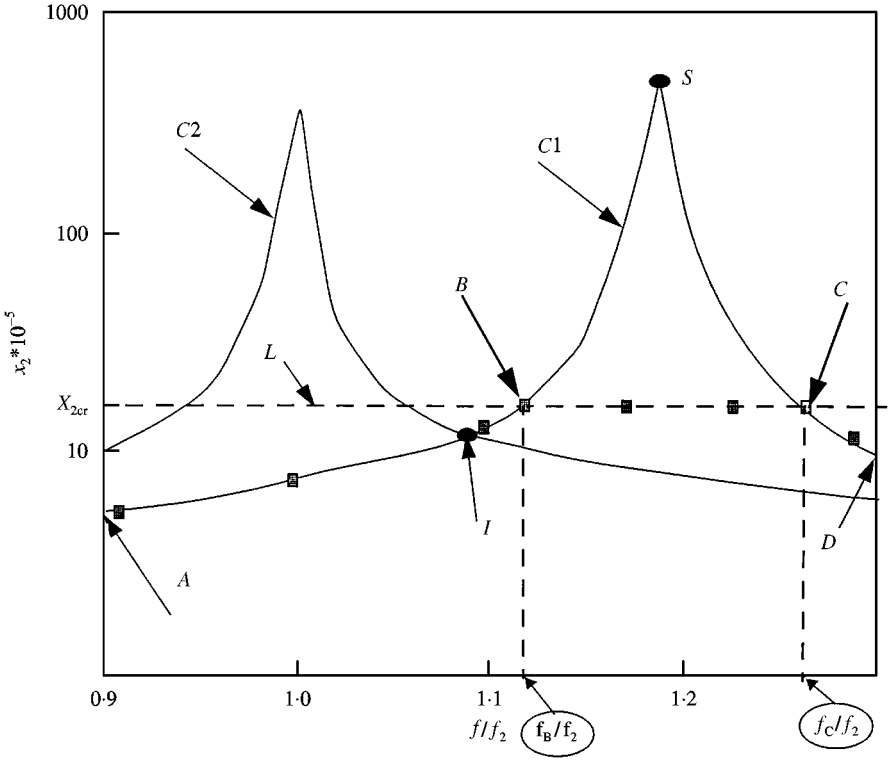

Figure 5. Variation of the amplitude X_2 with frequency ratio for $P > P_{cr}$. ■ Non-linear simulation.

state analysis. Thus, for this range of effort, the friction peak limiter is remarkably efficient because it does not allow the system to stay in either the sliding or the stuck mode. A phase difference appears, which limits the energy supplied to the system. It is this phenomenon which is at the root of the system's efficiency.

4.3. THIRD LOADING CONFIGURATION

Finally, let us consider a loading amplitude, such that points S and I are now above the critical sliding value (see Figure 6). For excitation frequencies lower than f_B or greater than f_C, by using the previous reasoning, the system response is provided by the portions AB and CD of the curve C_1.

For an excitation frequency equal to f_B (point B), the system jumps to the sliding mode, and can now be maintained in this mode because the amplitude of mass m_2 is above the critical value X_{2cr}.

Thus for this frequency, a discontinuity BG, due to a change in boundary conditions, must appear on the response curve. The discontinuity found not only by non-linear calculation, but also in tests by Toufine [23], can thus be explained.

On the portion GH, the sliding mode must then maintain its position since the displacement of m_2 is greater than X_{2cr}. On the other hand, on the portion HC, behaviour with stick slip, must be similar to the preceding case.

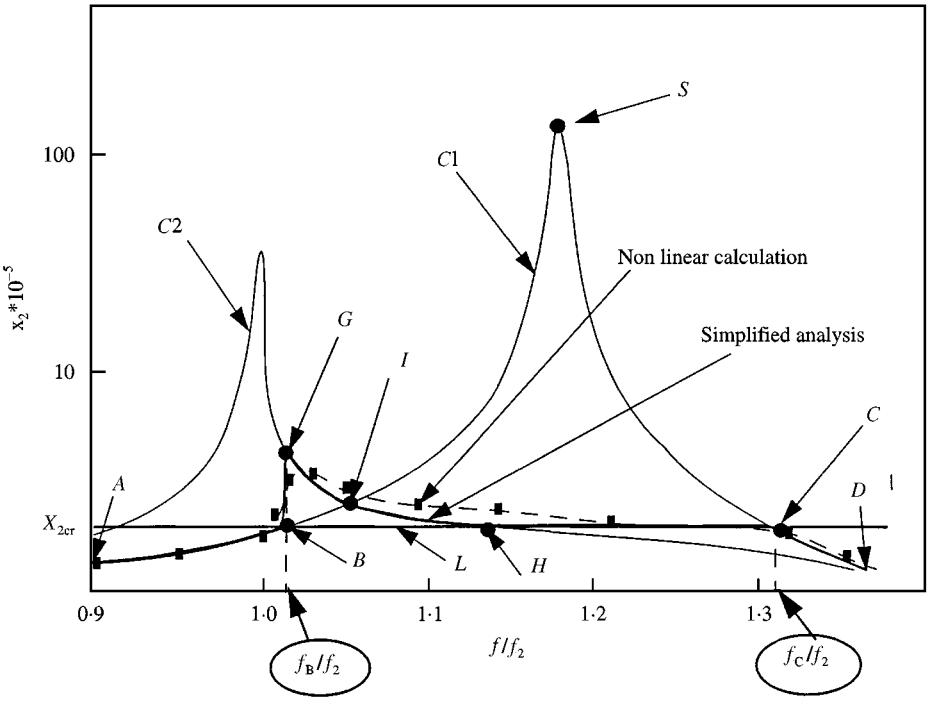

Figure 6. Variation of the amplitude X_2 with frequency ratio for $P \gg P_{cr}$.

With this analysis, system response should be provided by portions AB, BG, GH, HC and CD of the different curves C_1 and C_2 as shown in Figure 6. Here also, non-linear results give a response which is very near to those obtained by this analysis.

The peak-limiter efficiency curve enables us to see that for $P = 12$ N, point G is found at the beginning of the sliding quasi-linear zone of this curve. This point corresponds to point C in Figure 4.

The analysis of this loading configuration shows that the friction peak limiter is less efficient, but still prevents the system from remaining at the maximum value of the sliding response curve (see Figure 6). Only when the frequency associated with point B is less than the sliding mode frequency will the friction peak limiter lose all its efficiency.

In this case, the only interest of the system is the energy dissipated by friction, but this energy will rapidly become negligible compared with the energy lost by viscous damping, because viscous energy is proportional to the square of the amplitude, while energy lost by friction is simply proportional to the movement amplitude.

5. PARAMETERS AFFECTING THE DRY FRICTION INTERFACE

From this response, it is possible to understand the influence of various parameters and the interest of dry friction. Three cases of loading are thus considered.

5.1. LOADING $P < P_{CR}$

In this case, the system has a linear behaviour and the friction coefficient, μ_S, controls the value the critical force P_{cr}. As μ_S increases, as does P_{cr} and X_{1cr} (equation 3). For this loading, the efficiency curve gradient is linked to the viscous damping c_t and the friction peak limiter is no longer useful.

5.2. LOADING $P_{CR} < P$ AND $X_1 < X_{2CR} < X_S$

For this range of loading, the system is at maximum efficiency. Points I and S are situated on either side of the critical sliding value. The two important parameters that control the positions of these two characteristic points are

— the dynamic friction coefficient;
— the frequency difference between fundamental sliding and stuck modes.

Their effects on the system behaviour are analyzed in detail below.

Effects of the dynamic friction coefficient: To understand the effect of dynamic friction, the interface is considered as characterized by two friction coefficients: The static coefficient called μ_S and the dynamic coefficient called μ_d. Three values for the latter are considered: 0, μ_{d1} and μ_{d2}, with $0 < \mu_{d1} < \mu_{d2}$.

If the friction peak limiter efficiency curve is analyzed, point B in Figure 4 which characterizes the beginning of the plateau, is the same whatever the value of the dynamic coefficient, since its position is only linked to the static coefficient μ_S.

Now, with the coefficient μ_{d2}, the equivalent viscous damping C_{eq} is greater in equation 4 than with μ_{d1} and consequently the response curve of the sliding mode

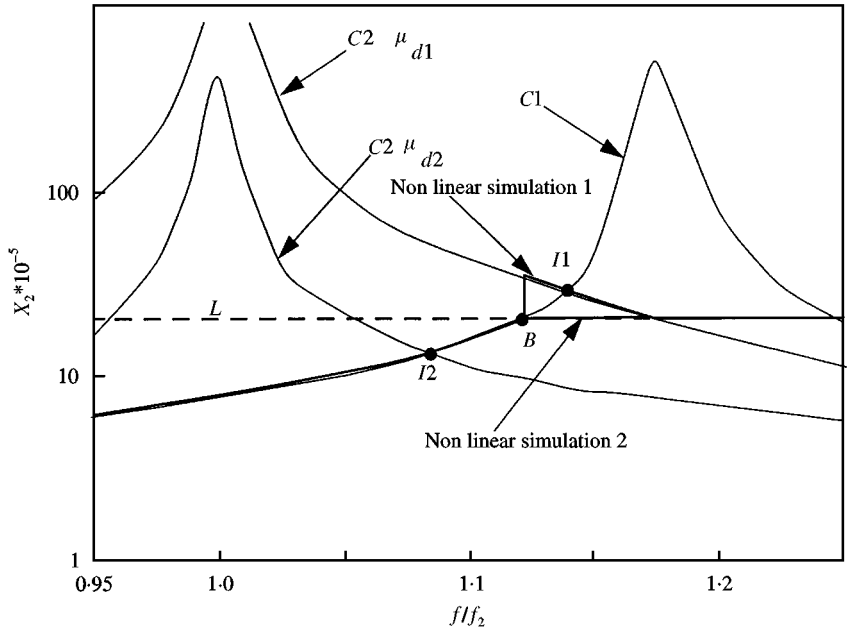

Figure 7. Variation of the amplitude X_2 with frequency ratio and dynamic coefficient μ_d.

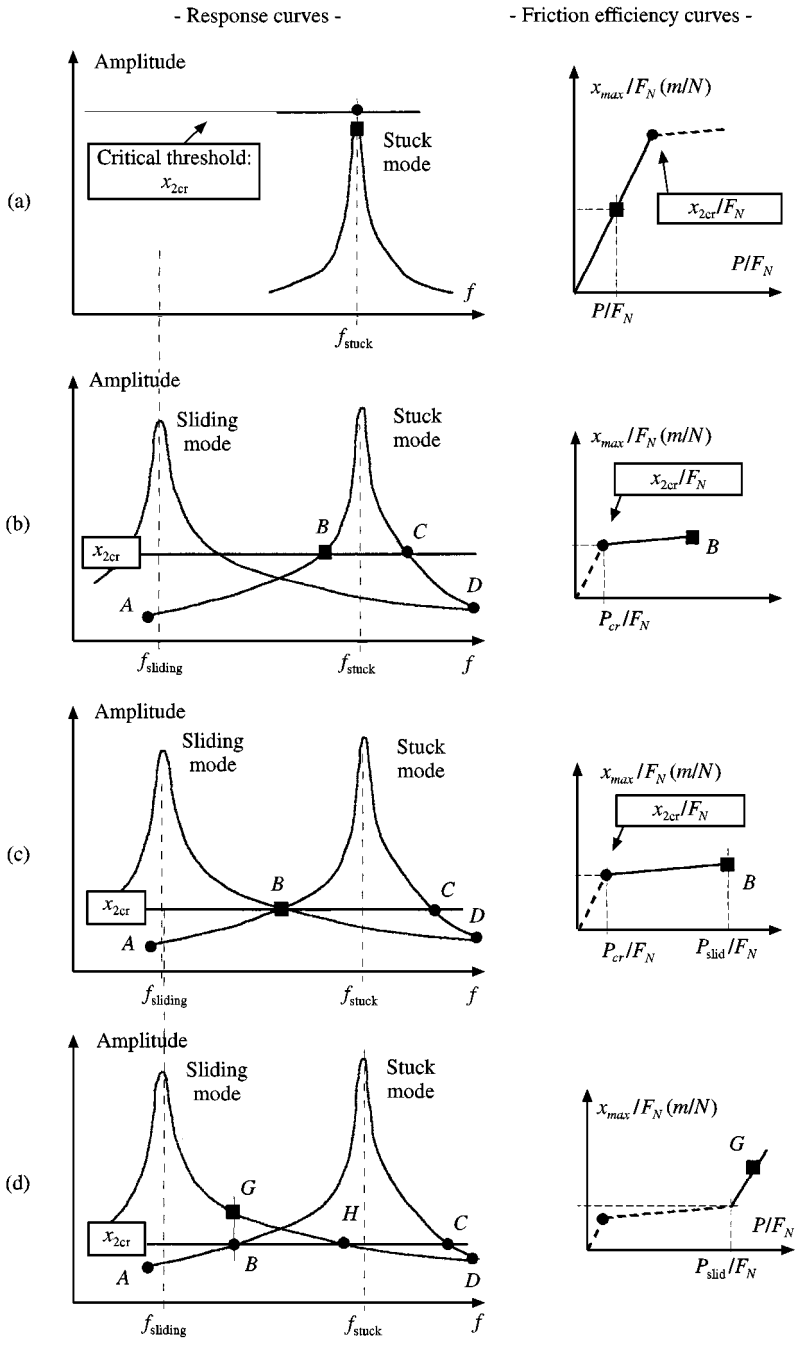

Figure 8. Global behaviour.

has a lower amplitude than that obtained with μ_{d1} in Figure 7. Thus, the intersection point I_2 associated with μ_{d2} is found to below the value X_{2cr}, while point I_1 associated with μ_{d1} is found to be above. Then for this excitation force, the maximum response amplitude associated with μ_{d2}, gives a point on the efficiency

curve situated on the plateau, while for μ_{d1}, the point is found in the quasi-constant sliding zone. Consequently, the length of plateau and the efficiency of the system increase as the value of μ_d becomes higher. Korkmaz had noted this effect of the coefficient μ_d on the system behaviour [24], but could not give any physical explanation.

Now we can analyze the case where the coefficient μ_d is zero and the coefficient μ_S is different from zero. In this case, the two points I and S can be found on either side of the critical value if the frequency difference between the two sliding and stuck modes is sufficient, and therefore the peak limiter efficiency curve plateau still exists.

As Korkmaz indicated without being able to explain it, a friction peak-limiter efficiency exists, even without dissipation of energy; the essential physical phenomenon is the change of boundary conditions that introduces phase differences and limits energy provided to the system. The friction peak limiter is efficient, not because of the energy that it dissipates, but because of the fact that it prevents energy from being supplied to the system.

Therefore, the dry friction coefficient μ_d is an important parameter for the friction peak limiter efficiency only when the two stuck and sliding modes are very close. In this case, as the coefficient μ_d increases, so does the length of the curve efficiency plateau.

In a real structure, the sliding mode is often fixed by design. To obtain a high-efficiency zone of the friction peak limiter, it is necessary for point I to remain under the line L. Clearly, the best solution consists of moving the stuck mode away from the sliding mode.

5.3. LOADING $P_{CR} < P$ AND $X_{2CR} < X_I < X_S$

For these forces, the curve gradient is linked to the energy dissipated by friction and by viscous damping. The latter rapidly becomes predominant compared with energy lost by dry friction, since it is proportional to the square of the amplitude while the former is simply proportional to the amplitude. In this case the system is not a really efficient means of reducing vibration.

6. CONCLUSION

Analysis of the simplified system shows that the friction peak limiter is efficient only for a given loading range.

System behaviour can be summarized in Figure 8, where three behaviour patterns appear associated with three ranges of forces:

(1) An initial loading where the amplitude of the excitation force is less than P_{cr}. The response is simply given by the stuck mode curve and the problem is linear (see Figure 8(a)).
(2) A second loading zone which begins for $P > P_{cr}$ and where points S and I are on either side of the line L defined by X_{2cr}. For this loading, the friction peak

limiter is highly efficient, because the boundary conditions of the system change. They pass successively from the stuck mode to the sliding mode (Figure 8(b)). In this configuration, the energy provided to the system is limited. Therefore, the friction peak limiter can be efficient, even without energy dissipation.

For this range of effort the maximum response amplitude corresponds to a point on the efficiency curve which is situated on the plateau.

The boundary is reached at a force P_2 when the point of intersection of stuck and sliding response curves cross in the vicinity of the critical sliding value (Figure 8(c)).

(3) A third zone of force occurs when $P > P_2$, when the friction peak limiter loses its efficiency by letting the system switch to the sliding mode. Even if the friction peak limiter continues to dissipate energy, this energy rapidly becomes negligible in relation to that lost by viscous damping. In this case a significant gradient reappears on the efficiency curve (Figure 8(d)).

The study of the parameters shows that

- the friction peak limiter efficiency is high if the frequency difference between the sliding and stuck modes is large;
- the dynamic friction coefficient is an important parameter only when the frequency difference between the two mode is high.

These results can not only be incorporated into structural design but can also improve the speed of numerical resolution methods since forces P_{cr} and P_2 can be obtained rapidly.

REFERENCES

1. J. P. Hartog 1931 *American Society of Mechanical Engineers Journal of Applied Mechanics* **53**, 107–105. Forced Vibrations with combined Coulomb and viscous friction.
2. M. S. Hundal 1976 *Journal of Sound and Vibration* **64**, 371–378. Response of a base excited system with Coulomb and viscous friction.
3. J. H. Griffin 1980 ASME *Journal of Engineering Power* **102**, 329–333. Friction damping of resonant stresses in gas turbine engine airfoils.
4. W. Ostachowicz 1989 *Journal of Sound and Vibration* **131**, 465–473. The harmonic balance method for determining the vibration parameters in damped dynamic systems.
5. E. H. Dowell and H. B. Schwartz 1983 *Journal of Sound and Vibration* **91**, 255–267. Forced response of a cantilever beam with a dry friction damper attached I Theory.
6. E. H. Dowell and H. B. Schwartz 1983 *Journal of Sound and Vibration* **91**, 269–291. Forced response of a cantilever beam with a dry friction damper attached II Experiment.
7. A. A. Ferri 1985 *A dissertation Presented to the Faculty of Princeton University in Candidacy for the Degree of Doctor of Philosophy, september* 1985. The dynamics of dry friction damped systems
8. A. Ferri and E. H. Dowell 1988 *Journal of Sound and Vibration* **124**, 207–224. Frequency domain solutions to multi-degree-of freedom, dry friction damped systems.
9. T. M. Cameron and J. H. Griffin 1989 *ASME Journal of Applied Mechanics* **56**, 149–154. An alternating frequency time domain method for calculating the steady-state response of nonlinear dynamic systems.

10. A. Cardona, T. Coune, A. Lerusse and M. Geradin 1994 *International Journal for Numerical Methods in Engineering* **37**, 1593–1608. A multiharmonic method for non-linear vibration analysis.
11. I. Korkmaz, J. J. Barrau, M. Berthillier and S. Crézé 1995 *Design Engineering Technical Conferences, the* 15*th Biennial Conference on Mechanical Vibration and Noise, September* 17–20, 1995, *Boston, Massachusets. DE-Vol. 84-1, Vol. 3-Part A, 1117–1124 in Proceedings of the 1995*. Theoretical dynamic analysis of a cantilever beam damped by a dry friction damper.
12. C. H. Menq, J. Bielak and J. H. Griffin 1986 *Journal of Sound and Vibration* **107**, 279–293. The influence of microslip on vibratory response, Part 1: a new microslip model.
13. A. Toufine *et al.* 1998 *Nonlinear Dynamics* pp. 1–17. Dynamic study of a structure with flexion-torsion coupling in the presence of dry friction.
14. C. H. Menq, J. H. Griffin and J. Belak 1986 *Journal of Sound and Vibration* **107**, 295–307. The influence of microslip on vibratory response.
15. K. Y. Sanliturk and D. J. Ewins 1996 *Journal of Sound and vibration* **193**, 511–523. Modelling two-dimensional friction contact and its application using harmonic balance method.
16. A. Girard and N. Roy 1997 *Revue Européenne des éléments finis* **6**, 233–254. Modal effective parameters in structural dynamics.
17. M. Berthillier, C. Dupont, R. Mondal and J. J. Barrau 1998 *Journal of Vibration and Acoustics* **120**, 466–474. Blades forced response analysis with frictions dampers.
18. A. Toufine, J. J. Barrau and M. Berthillier 1996 *Revue du GAMI*: *Mécanique Industrielle et Matériaux* **49**. Dynamic analysis of turbo prop engine blade with dry friction.
19. J. F. Ferrero and J. J. Barrau 1997 *Wear International Journal on the Science and the Technology of Friction and Wear* 58–61. Study of dry friction under small displacements and near zero sliding velocity.
20. J. H. Wang and W. L. Shieh 1991 *Journal of Sound and Vibration* **149**, 137–145. The influence of a variable friction coefficient on the dynamic behavior of a blade with a friction damper.
21. J. R. Anderson and A. A. Ferri 1990 *Journal of Sound and Vibration* **140**, 287–304. Behavior of a single degree of freedom system with a generalized friction law.
22. G. N. Vanderplaats 1984 *Numerical Optimization Techniques for Engineering Design: With Applications.* New York: McGraw-Hill.
23. A. Toufine 1997 *Thèse de doctorat ENSAE*. Dynamique de structures en présence de frottement sec: application aux aubes de turboréacteurs.
24. I. Kormaz 1993 *Thèse de doctorat ENSAE*. Contribution à l'étude d'une aube soumise à un frottement sec.

APPENDIX: NOMENCLATURE

C_{eq}	equivalent viscous damping
f	frequency in Hertz
F_N	normal force
F_T	tangential force
k_t	spring constant
P	applied force
X	displacement
$\dot{X}$	velocity
μ_d	dynamic friction coefficient
μ_s	static friction coefficient
ω	frequency in rad/s